Influence of Transmural Slow-Conduction Zones on the Long- Time Behaviour Of Atrial Arrhythmia. A Numerical Study with a Human Bilayer Atrial Model.

Simon Labarthe [1,2,3], Edward Vigmond[1,2], Yves Coudiere[1,2,3], Jacques Henry[1,2,3], Hubert Cochet[2,4], Pierre Jaïs[2,4]

[1] Lab IMB, University of Bordeaux 1 and Bordeaux Segalen, Talence, France
[2] Institut LIRYC, Pessac, France
[3] INRIA Bordeaux Sud Ouest, Talence, France
[4] CHU, Bordeaux, France

Abstract

Atrial fibrosis is known to be a factor in the perpetuation of atrial arrhythmia. Despite the thinness of atrial tissue, the fibrosis distribution may not be homogeneous through the entire thickness of the atria. This study aims to elucidate the respective influences of a transmural and a non-transmural distribution of fibrosis, described as a slow conduction zone, on the perpetuation of an arrhythmic episode, compared to a control situation. We used a bilayer monodomain representation of the atria that included transmural heterogeneities of fibre organisation. This model allowed long simulations for a sustainable computational load. We observed that when the fibrosis was transmural, the centre of the rotor was anchored in the slow conduction zone and was stable during a 10 seconds simulation, whereas the other simulations showed meandering rotors that disappeared after a few seconds. This study provided insight into the influence of transmural fibrosis on atrial arrhythmia perpetuation. In our model framework, only a transmural fibrosis distribution had a stabilizing effect on reentrant circuits. The bilayer model proved to be a good trade-off between accuracy and speed for observing the influence of transmural heterogeneities on atrial arrhythmia over long periods.

1. Introduction

Atrial fibrosis is known to be part of a negative loop occurring during atrial fibrillation (AF) [1] : persistant AF triggers structural remodelling, including the development of atrial fibrosis, which promotes arrhythmogenic propagation and begets AF. Although thin walled, physiological evidence of transmural heterogeneities in the atria are documented, such as abrupt variations of the fibre structure through the thickness[2] and electrical dissociation [1]. Measuring thickness of fibrotic scars is difficult in clinic due to spatial resolution of MRI. Furthermore, the functional consequences of scar transmurality are unknown.

The major aim of this study is determine the influence of a homogeneous representation of fibrosis across the thickness of the tissue compared to a transmurally heterogeneous fibrotic region, or normal tissue, on the perpetuation of arrhythmia. An answer to this question would give an insight into the role of fibrosis in reentry dynamics, and determine if it is a target for ablation therapy.

However, a good representation of the fibrosis is required in numerical models. This implies investigating how to take into account the microscale heterogeneities of the fibrotic structures in a tissue scale model of the atria as well as being aware of the limitations of the particular modelling strategy employed. As a secondary aim of this study, we also investigate such a limitation. This question is related to the necessary level of complexity of atrial models. Surface or volume models of the atria are generally used, depending on the trade-off between the computational load and the model precision required for a given application [3]. Transmural phenomena can not be modelled by surface models so we propose a bilayer approach that extends the usual surface models to allow transmural differences while keeping computational load low.

2. Method

Our model is based on a detailed bisurface model of human atria previously published [4] that we present briefly. We then introduce a bilayer version of the monodomain equation and indicate the method used for the comparison of the influence of transmural and non transmural fibrosis.

2.1. Geometry and fibres

The geometrical construction of the atria followed a rule-based semi-automatic method [5]. A geometry of

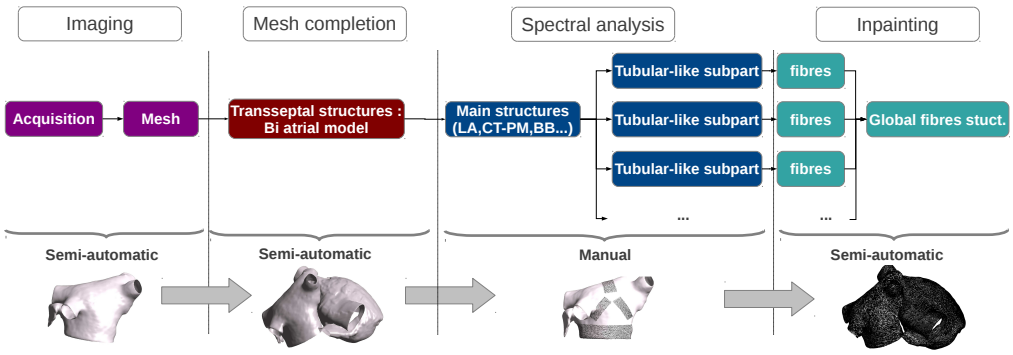

Figure 1. Work-flow of the fibres construction method.

the two chambers of the atria was first acquired using multi-detector computed tomography (MDCT) and meshed. Transseptal structures were semi-automatically constructed [4]. Then, fibre directions were added to the geometry by first constructing the anisotropy on cylinder-like structures where the fibre architecture is known to be circumferential, with a spectral analysis technique on a tensor of inertia. Fibre directions were completed in the whole atria with an inpainting algorithm.

We made several assumptions for our model. We first chose to represent the left atrium (LA) by implementing different fibres directions for the epicardic and endocardic surfaces following a histological study [2]. On the contrary, the right atrium (RA) is modelled with one layer for the whole chamber, completed by a second layer for the *crista terminalis* (CT) and the pectinate muscles (PM), the fibre direction of which is constructed following histological descriptions [6]. A block zone is included close to the sino-atrial node (SAN) [7]. Three transseptal structures are then added to electrically connect the RA and the LA : Bachmann's bundle (BB), the coronary sinus, and the conducting rim of the *fossa ovalis*. That resulted in a mesh containing 361483 nodes and 715034 elements with a mean diameter of 0.492 mm.

2.2. Mathematical model

The bilayer model is based on a bilayer version of the monodomain equation which has been derived from an asymptotic analysis of a 3D model [8]. That reads, in the layers $k = 1, 2$:

$$\beta(C_m \partial_t u^{(k)} + I_{ion}(u^{(k)}, v^{(k)})) = div_x(\sigma'^{(k)} \nabla_x u^{(k)}) + (-1)^k \sigma_c (u^{(1)} - u^{(2)}) \quad (1)$$

where $u^{(k)}$ (mV) and $v^{(k)}$ are respectively the transmembrane potential and the gate variables of the ionic model I_{ion} ($\mu\mathrm{A\,cm^{-2}}$). The tensor $\sigma'^{(k)}$ ($\mathrm{mS\,cm^{-1}}$) is a bi-dimensional diffusion one, whereas div_x and ∇_x are the classical bi-dimensional derivative operators. The coupling coefficient σ_c ($\mathrm{mS\,cm^{-2}}$) can be tuned to account for a given physiological thicknesses h (cm) — cf. [8]. In that version, the layers are defined on the same geometric surface.

A discrete version of this equation needs a specific implementation in solvers specifically dedicated to cardiac electrophysiology. To avoid this difficulty, we constructed a second surface at a constant distance ϵ from the first one and we added linear elements of section S between the nodes of both structures. A finite element semi-discrete version of that implementation can be written:

$$\beta \left(M_k + \frac{\epsilon |S|}{2} Id \right) \left(C_m \partial_t U^{(k)} + I_{ion}(U^{(k)}, V^{(k)}) \right) = - K_k U^{(k)} + (-1)^k \frac{|S|}{\epsilon} \sigma_L \left(U^{(1)} - U^{(2)} \right) \quad (2)$$

where M_k and K_k are the mass and stiffness matrix of the geometry $k = 1, 2$, and σ_L ($\mathrm{mS\,cm^{-1}}$) is a diagonal matrix that collects the different conductivity values on the linear elements and $|S|$ is the surface of the section of the linear elements. If ϵ is sufficiently small, one can check that $M_1 \simeq M_2$, $K_1 \simeq K_2$ and that the two approaches are equivalent when $\frac{|S|}{\epsilon} \sigma_L = \sigma_c M_1$.

We implemented this second method with the solver CARP [9] with a fixed time step of 25 µs using a Crank-Nicolson scheme.

2.3. Electrophysiological parameters

β and C_m are respectively set to $1400 cm^{-1}$ and $1\mu\mathrm{F\,cm^{-2}}$.We used the CRN model, that we modified to model a functional remodelling (multiplication by 1.45 and 0.65 of, respectively, the Kr and Ca, l channel conductances) and to get a correct tissue wave length (multiplication by 1.5 of g_{Na}, except for the BB where the factor was 2.5). We also applied 10 stimulations at a bcl of 300 ms before the simulation to enhance the inductibility

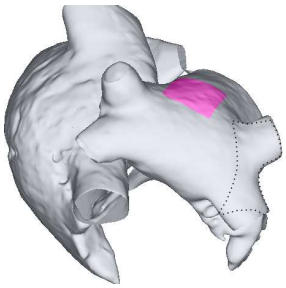

Figure 2. Slow conduction zone (pink area) in the posterior wall of the LA and S2 stimulation zone (dashed line)

of arrhythmia. A passive model is set in the block zone near the SAN. The longitudinal and transverse bidimensional conductivities are set to 0.3 and 0.04 $\mathrm{S\,m^{-1}}$, except on the CT and PM where the longitudinal conductivity is set to 1.0 $\mathrm{S\,m^{-1}}$. ϵ was set to 100 µm, $|S|$ to 1 $\mu\mathrm{m}^2$ and σ_L to 20 $\mathrm{S\,m^{-1}}$. A S1-S2 protocol was defined to trigger a macro-reentry in the ostial part of the left pulmonary veins (cf. figure 2 to see the S2 stimulation zone). Ectopic sources are defined in the right superior pulmonary vein and in the two left pulmonary veins after the S2 stimulation, and bursting at a respective bcl of 175, 200 and 235 ms to sustain the arrhythmic activity.

The slow conduction zone was modeled by setting the multiplication factor of g_{Na} to 1.0, and the longitudinal and transverse conductivities to 0.08 and 0.02 $\mathrm{S\,m^{-1}}$. Three fibrotic configurations are defined. The **transmural configuration** is constructed by taking those parameters on the area presented in the figure 2 and on both layers. The **non transmural configuration** is defined by taking those parameters also in that zone but only on the epicardial surface. The **control configuration** is set by keeping the initial parameters.

2.4. Comparison criteria

We performed a 10 s simulation for each fibrotic configuration. We compared the delay when no rotor could be observed on the atria, i.e., when the electrical wave spread regularly from one of the stimulation sources in the pulmonary veins towards the rest of the atria.

3. Results

A macro reentry with a eight shape was initially triggered in all fibrotic configurations after the S2 stimulation. The propagation sequence was then different.

In the transmural configuration, a functional bloc in one of the branch of the macro-reentry triggered a rotor in the posterior wall of the LA. The core of this rotor was rapidly anchored in the slow conduction zone and kept stable during the whole simulation (cf. figure 3), despite the perturbations coming from the ectopic sources. In the non transmural configuration, a functional bloc also begeted a rotor in the posterior wall of the LA. The motion of the core of this rotor was not limited to the slow conduction zone but moved through a large part of the posterior wall. After 5.01 s, the rotor stopped and the electrical activity became regular and was only leaded by the pulmonary veins. The control configuration gave a result similar to the non transmural configuration : a rotor coming from the inital reentry gave large drifts in the LA wall and stopped after 5.96 s. A $1\mathrm{s}$ simulation took $5296\mathrm{s}$ using 16 cores.

4. Discussion and conclusion

In this study, a fully transmural distribution of fibrosis allowed a rotor core which entered the fibrotic zone to attach itself there. That stabilized the reentry and allowed its perpetuation during the 10 s of simulation. When the fibrosis was not transmural, the reentry did not stay ancored, and vanished after a few seconds. A strong alteration of the tissue, particularly transmural, seems to have a stabilizing effect on the arrhythmia.

Neither the patch of fibrotic tissue nor the initial macro reentry included in that study are physiological. This idealised fibrotic configuration and stimulation protocol gave a quite organised reentrant arrhythmia. The arrhythmic dynamics would be more complex in a heterogeneously remodelled physiologic tissue. However, we postulate that the stabilizing effect of a transmural distribution of fibrosis in a more complex situation would remain.

Furthermore, if an acquisition of a patient dependant atrial fibrosis can be approached with a late-enhancement-MRI sequence, this image is only defined on a mean surface of the atria. No evaluation of the transmural distribution of fibrosis is possible. Then, projecting this surface distribution of fibrosis homogeneously in the thickness of the atria may lead to introduce artificially this stabilizing effect and to a more arrhythmic model.

The bilayer model of the atria that we developed allowed to include transmural heterogeneities in a surface model, further letting us simulate three dimensional behaviours with a bidimensional computational load during long simulation times. This study demonstrates the potential of the bilayer approach.

Acknowledgements

The research leading to these results has received funding from the European Union Seventh Framework Programme (FP7/2007-2013) under Grant Agreement HEALTH-F2-2010-261057. Experiments presented in this paper were carried out using the PLAFRIM experimental testbed, being developed under the Inria PlaFRIM develop-

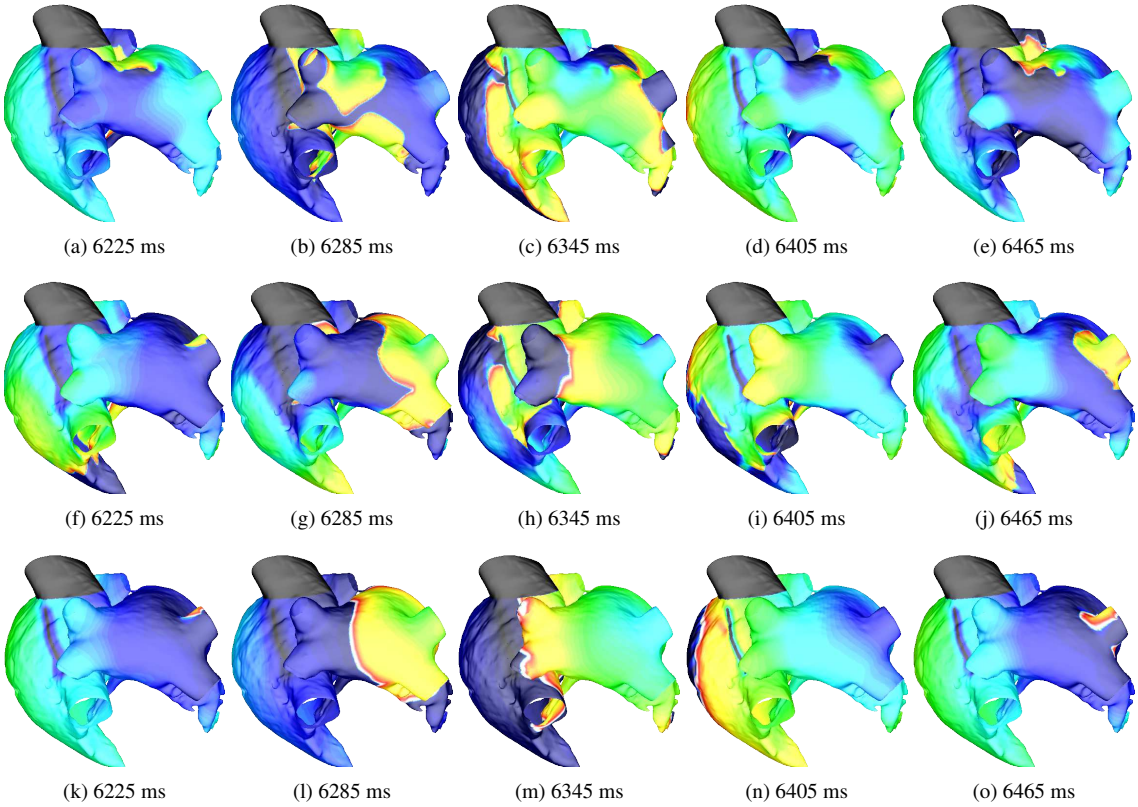

(a) 6225 ms (b) 6285 ms (c) 6345 ms (d) 6405 ms (e) 6465 ms

(f) 6225 ms (g) 6285 ms (h) 6345 ms (i) 6405 ms (j) 6465 ms

(k) 6225 ms (l) 6285 ms (m) 6345 ms (n) 6405 ms (o) 6465 ms

Figure 3. Snapshots of the propagation sequence of the transmural configuration (a)-(e), non transmural configuration (f)-(j) and control(k)-(o). We can see that the rotor is still stable after 6.2 s in the posterior wall of the LA in the transmural configuration and that the core is located in the slow conduction zone. In the other situation, no rotor can be observed.

ment action with support from LABRI and IMB and other entities: Conseil Régional d'Aquitaine, FeDER, Université de Bordeaux and CNRS. This work was supported in part by the government of France through the ANR Investissements d'Avenir grant ANR-10-IAHU-04.

References

[1] Schotten U, Verheule S, Kirchhof P, Goette A. Pathophysiological mechanisms of atrial fibrillation: A translational appraisal. Physiological Reviews 2011;91(1):265–325.

[2] Ho S, Sanchez-Quintana D, Cabrera J, Anderson R. Anatomy of the left atrium: implications for radiofrequency ablation of atrial fibrillation. Journal of Cardiovascular Electrophysiology 1999;10(11):1525 – 1533. ISSN 1045-3873.

[3] Dössel O, Krueger M, Weber F, Wilhelms M, Seemann G. Computational modeling of the human atrial anatomy and electrophysiology. Medical Biological Engineering Computing 2012;50:773–799. ISSN 0140-0118.

[4] Labarthe S, Vigmond E, Coudière Y, Henry J, Cochet H, Jais P. A computational bilayer surface model of human atria. In FIMH 2013, Lecture Notes In Computer Sciences. S.Ourselin, D.Ruecker, N.Smith, London, United Kingdom: Springer, March 2013; .

[5] Labarthe S, Coudière Y, Henry J, Cochet H. A semi-automatic method to construct atrial fibre structures : a tool for atrial simulations. In CinC 2012 - Computing in Cardiology, volume 39. Krakow, Pologne, November 2012; .

[6] Ho SY, Anderson RH, Snchez-Quintana D. Atrial structure and fibres: morphologic bases of atrial conduction. Cardiovascular Research 2002;54(2):325–336.

[7] Fedorov VV, Schuessler RB, Hemphill M, Ambrosi CM, Chang R, Voloshina AS, Brown K, Hucker WJ, Efimov IR. Structural and functional evidence for discrete exit pathways that connect the canine sinoatrial node and atria. Circulation Research 2009;104(7):915–923.

[8] Coudière Y, Henry J, Labarthe S. An asymptotic two-layers monodomain model of cardiac electrophysiology in the atria.

[9] Vigmond EJ, Hughes M, Plank G, Leon L. Computational tools for modeling electrical activity in cardiac tissue. Journal of Electrocardiology 2003;36, Supplement 1(0):69 – 74. ISSN 0022-0736.

Address for correspondence:

Simon Labarthe

Inria,200 avenue de la Vieille Tour, 33405 Talence Cedex, France

simon.labarthe@u-bordeaux2.fr